

Inversion for Source Wavelet and AVA parameters from Prestack Seismic Data

Partha S. Routh, Phil D. Anno and Robert T. Baumel (ConocoPhillips, Seismic Imaging and Prediction Center, Houston, Texas USA), J. Andres Chavarria (Duke University, Durham, North Carolina USA)

Summary

It is difficult to establish the influence of the seismic wavelet on reflection data away from well control. In this paper we present an inversion methodology to extract a source wavelet from a prestack gather. This inversion estimates and deconvolves the effective source contribution, at the same time estimating reflectivity with high resolution. Discrimination of source from reflectivity depends on differential, that is, non-parallel, moveout over offset.

The reflection data depend nonlinearly on the unknowns when one seeks both a source and a reflectivity function. Moreover, limitations from data sampling produce an ill-conditioned system of equations to solve. We therefore treat this inverse problem as underdetermined. We also compute a solution involving different norms for the wavelet and AVA parameters. This overall design helps imprint physically intuitive characteristics on the solution.

Our inversion examples demonstrate that the algorithm is robust. In our synthetic test we recover a non-minimum phase wavelet and AVA parameters to within a scale factor. In our field data example we obtain a consistent source wavelet from each CIP gather, and the inverted intercept-gradient parameters have better resolution than the stack.

Introduction

Wavelet estimation and deconvolution is always an important part of seismic data processing and interpretation. The processing-oriented approaches usually make assumptions about wavelet phase and/or the statistics of reflectivity (Robinson, 1967; Ulrych et al., 1995; Lazear, 1993). Interpreters rely more on direct knowledge of the earth's reflectivity. They often perform wavelet extractions based on borehole-derived synthetics or reflections from a water bottom or salt. Ziolkowski (2000) discusses direct measurement of the source signature. This procedure can be effective for designature in a deepwater marine environment.

In this paper we present a practical inversion methodology to estimate both a source wavelet and, simultaneously, AVA parameters from a multioffset gather. This alternative avoids questionable assumptions about wavelet phase and reflection statistics. And it is feasible in all acquisition environments, land or marine. However, this inversion does not circumvent entirely the need for reflectivity information, as multioffset data alone do not resolve wavelet polarity. One must

therefore independently introduce the correct wavelet polarity (equivalently, the correct reflectivity polarity) if it is critical to the interpretation.

This inverse problem was investigated by researchers from The Rice Inversion Project (Minkoff and Symes, 1997). In our paper we formulate the inversion as a time-domain rather than depth-domain process. We view any required depth-domain processing as preprocessing for our algorithm. This includes assuming the velocity field is known from other analysis. We also parameterize reflectivity in terms of intercept and gradient, rather than an arbitrary function of reflection angle. These considerable simplifications greatly improve compute cost, robustness, and uniqueness of the solution.

Demonstrated by Winslow et al. (2000), this inversion depends on the nonparallel moveout of reflection events. This is the data information that distinguishes interfering wavelets from angle-dependent reflectivity. The greater the effective aperture at an event, the more the multioffset data constrain the solution. In order to honor physical intuition where the data constraint is poor we utilize a different norm for the source than for reflectivity. We expect the wavelet to be a smooth, oscillatory function. In contrast to the source, our norms for intercept and gradient predispose reflectivity solutions to be sparse and discontinuous.

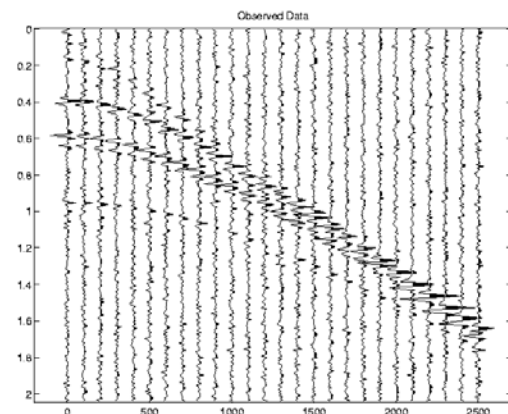


Figure 1. Synthetic data generated with the source wavelet in Fig. 3(a), AVA parameters in Figs. 2(a) and 2(b), and Gaussian random noise. The horizontal coordinate shows offsets from 0-2500 m, the vertical coordinate is time (s).

Nonlinear Inversion of Prestack Data

Synthetic Example

Primary inputs to our algorithm are a CIP gather with its moveout velocity function. Figure 1 shows a synthetic input gather. These data were computed from intercept and gradient models in Figures 2a and 2b. The source (Figure 3a) is a time-shifted, 30 Hz Ricker wavelet with linear phase. A typical velocity function was used to impart moveout in the data over offset.

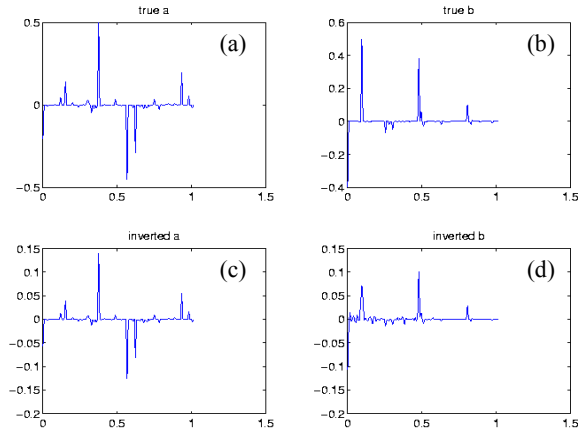


Figure 2. Comparison between true intercept a and gradient b (panels (a) and (b)) with inverted parameters (panels (c) and (d)). The horizontal coordinate is zero-offset time, in seconds, in each graph.

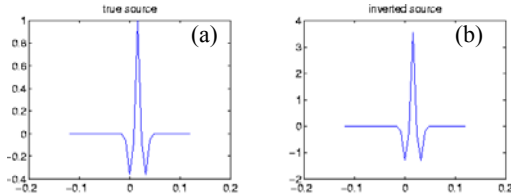


Figure 3: Comparison between the true wavelet and the inverted wavelet. The horizontal coordinate is time (s). The inverted wavelet matches well with the true wavelet, modulo a scale factor.

Figure 3b plots the source wavelet recovered from inverting the synthetic gather. The recovered source matches well with the true wavelet to within a constant scale factor. Numerous other synthetic tests with mixed-phase wavelets show that the algorithm accurately recovers phase.

Recovered intercepts (Figure 2c) and, to a lesser extent, gradients (Figure 2d) also compare favorably with the true parameters. Prestack data are less sensitive to gradient than intercept, making small gradients more difficult to recover

from events with poor signal-to-noise ratio.

Secondary inputs for our algorithm include reference and starting models for the wavelet as well as for intercept and gradient. In this example we chose these models to be small constants close to zero. These particular choices imply a complete absence of a priori information about the wavelet or reflectivity. Another input parameter, however, bounds intercept and gradient solutions to lie within a specified range. We chose $-.6$ to $.6$ for the bounds in this example. The source wavelet length parameter was set to $.24$ s.

Forward Modeling

Equation (1) parameterizes our earth model for reflectivity in terms of intercept (a) and gradient (b). Coordinates of the model are given in zero-offset time, t_0 . Reflection angle is denoted by θ . Though different, or more, model parameters could be considered we recommend significantly fewer parameters than offsets. This constraint brings to bear experience with AVA methods, increases robustness, and decreases compute cost.

$$r(t_0, \theta) = a(t_0) + b(t_0) \sin^2 \theta. \quad (1)$$

$$u(t, h) = s(t) * r(t, h). \quad (2)$$

Equation (2) expresses our modeling operator for CIP data -- the time convolution of a source wavelet $s(t)$ with $r(t, h)$, offset-dependent reflectivity. Equations (3) and (4) define the mapping of reflectivity, called for by equation (2), from model coordinates and angles to data coordinates (t, h) .

$$r(t, h) = \int_{t_0^{\min}}^{t_0^{\max}} dt_0 r(t_0, \theta(t, h)) \delta(t - \tau(t_0, h)), \quad (3)$$

$$\tau(t_0, h) = \sqrt{t_0^2 + h^2 / V^2(t_0)}. \quad (4)$$

Forward modeling through equations (1)-(4) represents rather simple wave propagation. Data preprocessing is therefore always necessary to bring recorded input data into conformance with this type of model data.

Equation (2) illustrates the inherent ambiguity in polarity of the solutions. Multiplication of both source wavelet and reflectivity by -1 leaves data $u(t, h)$ unchanged. The CIP data therefore do not resolve polarity. This ambiguity can only be resolved by introducing either a wavelet polarity or a reflectivity polarity through independent information.

Nonlinear Inversion of Prestack Data

Inverse Problem

The inversion aims to recover three types of model parameters (source, intercept and gradient) from a multioffset gather. We pose this problem as underdetermined, with more parameters than data. There are more data in practice. But, around narrow-aperture events in the gather the data constraint is weak. This gives an ill-conditioned (rank-deficient) system of equations and an effectively underdetermined, nonunique solution at those coordinates.

We are free to impose our physical intuition where the constraints of data fall short. This is done through a suitably designed objective function. We minimize L1 norms involving intercept and gradient, based on our view that they should be spiky, discontinuous solutions over time. Conversely, we see a source wavelet as smooth and oscillatory and minimize an L2 measure instead. These minimizations are subject to keeping reflectivity within specified bounds and fitting the observed data to within a specified L2 tolerance.

A full-Newton interior point method accommodates our bounds on reflectivity and mixed norms on the model parameters. We implement the L1 norms via iteratively reweighted least squares. We solve the system of equations arising from minimization through a least-squares, conjugate gradient algorithm.

Field Example

Figure 4 shows a few of the CIP gathers input for inversion. Each gather contains 28 offsets, 225-3000 m. We inverted a window of data defined by upper and lower hyperbolic boundaries. These boundaries follow trajectories defined by the moveout velocity function, intersecting zero offset at .4 s and 1.7 s.

Output from this window of data consists of an effective source wavelet, length .24 s, with its associated intercept and gradient traces. Figure 5 presents representative wavelets from different gathers. The inverted wavelet is consistent from one gather to the next, with an effective length much shorter than the prescribed length.

Figures 7 and 8 demonstrate inverted intercept and gradient traces. These sections were formed by inverting CIP gathers from bins along a line through a 3D volume. Figure 6 shows the stack section, computed with the same velocity functions and offsets used for inversion. Figures 6, 7, and 8 were also post-filtered with identical bandpass filters.

The intercept section of Figure 7 shows the best effective bandwidth and resolution, followed next by gradient (Figure 8), then the stack (Figure 6). The bandwidth of the

stack suffers from normal moveout stretch. Conversely, source deconvolution increases resolution on intercept and gradient. This designature is inherent in inverting equation (2) for reflectivity. Our L1 descriptor for inverted traces, particularly gradient, also benefits resolution. The data constraint on gradient is less than for intercept, making this choice for the norm significant.

Important preprocessing for these field data included demultiple and anisotropic depth imaging. We applied a Radon-transform multiple attenuation procedure before inversion, as equations (1)–(4) model only primary reflections. Anisotropic imaging corrected the inversion input data for nonhyperbolic moveout (Meek et al., 2002). That is, the corrected data conform well to equation (4). One could also directly introduce an anisotropic moveout equation into the modeling operator, in place of equation (4). In either case, we recommend a final pre-inversion velocity analysis to ensure the accuracy of the input velocity field.

Conclusions

In this work we describe a nonlinear inversion method to estimate a source wavelet and intercept-gradient traces from each CIP gather. In our synthetic test we recover a non-minimum phase wavelet and these AVA parameters to within a scale factor. Our field trial extracts a consistent source wavelet from each gather. The associated intercept-gradient data show better resolution than the stack. We attribute this resolution to the inherent designature of the inversion and our particular choice of norms. We employ L2 norms for the source wavelet and data misfit, L1 norms for intercept and gradient.

References

1. Lazear, G. D., 1993, Mixed-phase wavelet estimation using fourth-order cumulants: *Geophysics, Soc. of Expl. Geophys.*, 58, 1042-1051.
2. Meek, R., Anno, P., Brewer, J., and Coral, M., 2002, Anisotropic velocity model building and updating for prestack depth migration in Indonesia, *SEG Expanded Abstracts*, Salt Lake City, 145-148.
3. Minkoff, S. E. and Symes, W. W., 1997, Full waveform inversion of marine reflection data in the plane-wave domain: *Geophysics*, 62, 540-553.
4. Robinson, E., 1967, Predictive decomposition of time series with application to seismic exploration: *Geophysics*, 32, 418-484.
5. Ulrych, T. J., Velis, D. R. and Sacchi, M. D., 1995, Wavelet estimation revisited: *The Leading Edge*, 14, no. 11, 1139-1143.
6. Winslow, N.W., Minkoff, S. E., and Symes, W. W., 2000, Source inversion: Not a miracle, *Rice Inversion*

Nonlinear Inversion of Prestack Data

Project report.

- Ziolkowski, A., 2000, Simplified wavelet estimation using source-signature measurements: The Leading Edge, 19, no. 01, 61-67.

Acknowledgements

We thank Bill Symes, of Rice University, who introduced us to their work on source inversion. Dale Cox helped us greatly with his insightful advice and software support. We thank Bob Corbin, Javaid Durrani and Baishali Roy for many helpful discussions. And we thank ConocoPhillips for permission to publish this work.

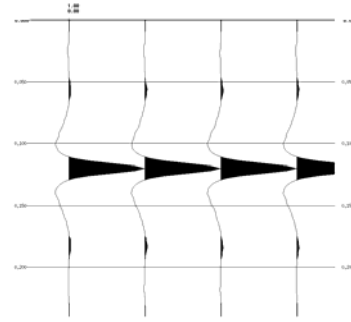


Figure 5. Representative source wavelets, output from inversion. Each wavelet derives from a different common image point gather.

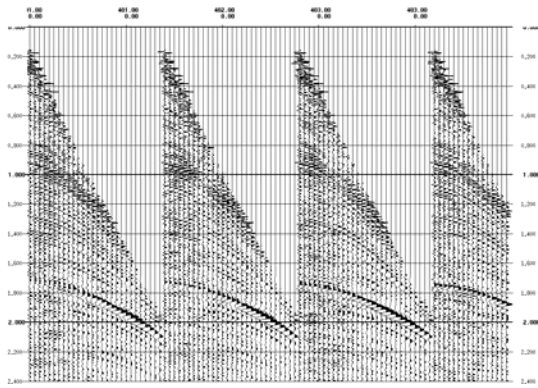


Figure 4. Representative common image point gathers, for input to inversion.

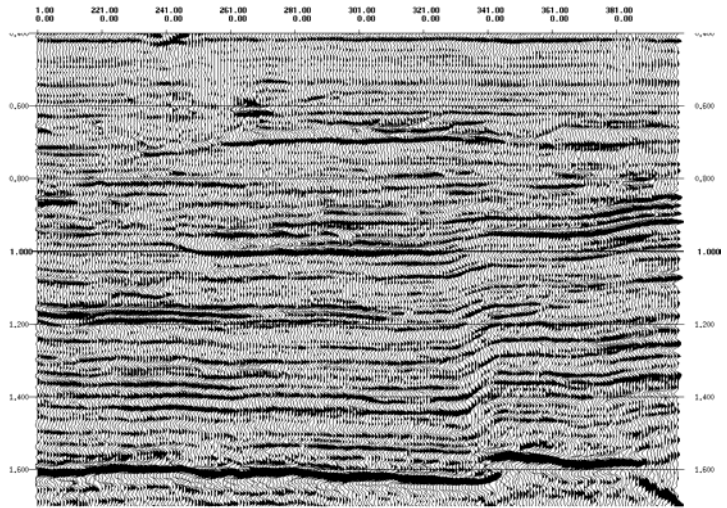


Figure 6. Stack section along a line through a 3D data volume.

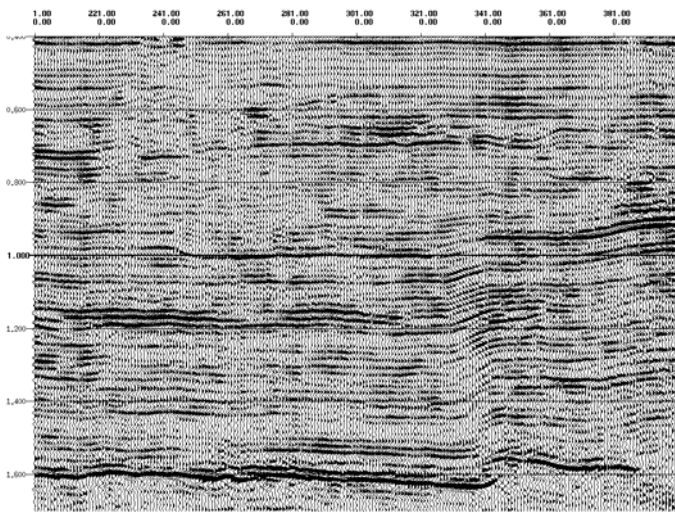


Figure 7. Intercept section from nonlinear inversion. This data exhibits greater bandwidth and resolution than the corresponding stack in Figure 6.

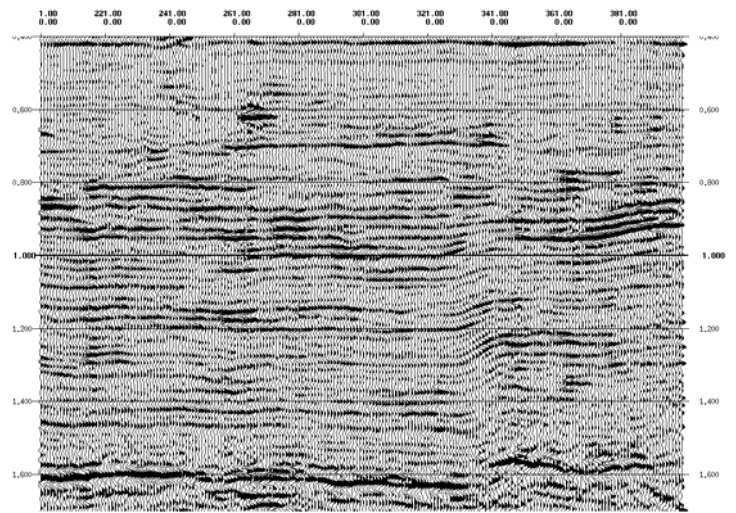


Figure 8. Gradient section from nonlinear inversion. This section shows greater resolution than the stack, but less than the intercept data in Figure 7.